AAC Accepted Manuscript Posted Online 29 July 2019
Antimicrob. Agents Chemother. doi:10.1128/AAC.00652-19

Title: Model-based Relationship between the Molecular Bacterial Load Assay and Time-to-Positivity in Liquid Culture

Running title: MBL-TTP pharmacometric model

Robin J Svensson,[1] Wilber Sabiiti,[2] Gibson S Kibiki,[3] Nyanda E Ntinginya,[4] Nilesh Bhatt,[5] Geraint Davies,[6] Stephen H Gillespie[2] and Ulrika SH Simonsson[1*]

[1]Department of Pharmaceutical Biosciences, Uppsala University, Uppsala, Sweden

[2]The School of Medicine, University of St. Andrews, St. Andrews, United Kingdom

[3]East African Health Research Commission, Arusha, Tanzania

[4]NIMR – Mbeya Medical Research Centre, Mbeya, Tanzania

[5]Instituto Nacional de Saúde (INS), Ministério da Saúde, Mozambique

[6]Department of Molecular and Clinical Pharmacology, University of Liverpool, Liverpool, United Kingdom

[*]Corresponding author: Ulrika SH Simonsson

Key words: pharmacometrics, pharmacodynamics, modelling, biomarker, tuberculosis

Abstract

The molecular bacterial load (MBL) assay is a new tuberculosis biomarker which provides results in ~4 hours. The relationship between MBL and time-to-positivity (TTP) has not been thoroughly studied and predictive models do not exist. We aimed to develop a model for MBL and identify the MBL-TTP relationship in patients. The model was developed on data from 105 tuberculosis patients from Malawi, Mozambique and Tanzania with joint MBL and TTP observations quantified from patient sputum collected for 12 weeks. MBL was quantified using polymerase chain reaction (PCR) of mycobacterial RNA and TTP using the Mycobacterial Growth Indicator Tube (MGIT) 960 system. Treatment consisted of isoniazid, pyrazinamide and ethambutol in standard doses together with rifampicin 10 or 35 mg/kg. The developed MBL-TTP model included several linked sub-models; a component describing decline of bacterial load in sputum, another component describing growth in liquid culture and a hazard model translating bacterial growth into a TTP signal. Additional components for contaminated and negative TTP samples were included. Visual predictive checks performed using the developed model gave good description of the observed data. The model predicted greater total sample loss for TTP than MBL due to contamination and negative samples. The model detected an increase in bacterial killing for 35 versus 10 mg/kg rifampicin (p=0.002). In conclusion, a combined model for MBL and TTP was developed that described the MBL-TTP relationship. The full MBL-TTP model or each sub-model used separately. Secondly, the model can be used to predict biomarker response for MBL given TTP data or *vice versa* in historical or future trials.

Introduction

The tuberculosis (TB) burden in patients is usually quantified by culture on solid medium or in liquid culture such as the Mycobacterial Growth Indicator Tube (MGIT) (1). In the diagnostic phase, the TB burden quantification gives information on disease severity and when collected during treatment, it gives information on treatment response. Quantification has usually been done using colony forming units (CFU) on solid media (2) or time-to-positivity (TTP) in liquid culture using MGIT system (1).

MGIT TTP has advantages over CFU counts on solid media by being less labour-intensive and more sensitive (3) but like CFU, TTP is hampered by a high degree of sample loss due to contamination and the long time taken before results are available (5-42 days) (4). This delay has a particular impact when quantitative methods are used in patient care where individual treatment adjustment decisions based on bacterial response should ideally be quick. Time-to-positivity is a time-to-event variable representing an indirect measurement of the bacterial load (high CFU gives short TTP).

The molecular bacterial load (MBL) assay is a new TB biomarker which is fast (~4 hours) (4) and has limited risk of contamination (5). This is because MBL is a non-culture-based real-time polymerase chain reaction (PCR) method relying on Reverse-Transcription quantitative PCR (RT-qPCR) of16S rRNA to quantify bacterial load (6). Viable TB cells contain 16S rRNA which makes MBL a continuous measurement of bacterial load. MBL can be used to predict bacterial load.

MBL has weak to moderate correlation with TTP in clinical trials with reported correlations of -0.5 (4) and -0.8 (7) using Spearman rank correlation. The weak correlation is not surprising since these biomarkers are different: MBL being a direct, continuous variable and TTP being an indirect, time-to-event variable. Non-linear mixed effects models have been

applied separately to MBL- (5) and TTP- (8–10) datasets separately but a combined MBL-TTP model has not been presented previously. The current TTP only models do not consider contaminated samples which are a common occurrence in culture-based detection of TB.

Identifying the link between MBL and TTP could contribute to the understanding of the difference in how these biomarkers quantify bacterial burden. A combined MBL-TTP model could also be used to predict one biomarker response given information about the other biomarker providing additional insights from historical trials. Given that, in some studies contamination is common especially later in treatment, including a component for contaminated TTP samples is warranted.

The objectives of this study were to develop a model for MBL and identify the relationship between MBL and TTP in pulmonary TB patients by constructing a joint MBL-TTP model.

Methods

Patient data

The model was developed on joint MBL and TTP observations collected repeatedly over the first 12 weeks of treatment in TB patients from an underlying study whose design and original findings are reported in detail in the relevant reference (11). Briefly, the dataset comprised of data from three clinical sites in Malawi, Mozambique and Tanzania with a total sample size of 105 patients (20, 53 and 32 patients from Malawi, Mozambique and Tanzania, respectively). For the current analysis, only patients with drug-susceptible TB were included. The Tanzania data were a subset of the MAMS-TB trial that has been described in detail elsewhere (12). All patients received rifampicin and isoniazid throughout the whole study. Rifampicin was given as 10 mg/kg in 93 patients and 35 mg/kg in 12 of the patients from MAMS-TB (12). Isoniazid was given in standard dosage (5 mg/kg). Ethambutol and pyrazinamide were given in standard dosage (15-20 and 20-30 mg/kg, respectively) for the first eight weeks. Sputum was collected at baseline and at weeks 2, 4, 8 and 12 at all three sites. Sputum sampling was done either by spot sampling where sputum was collected during the on-going visit or by early morning samples where sputum was collected over-night. Pooled spot and early morning sputum was used to determine MBL and TTP for Malawi and Mozambique. For Tanzania, MBL was quantified on spot and TTP on early morning sputum. The procedure for MBL quantification was identical between sites as described previously (7). Time-to-positivity was determined using MGIT 960 (Becton-Dickinson, Sparks, MD). The TTP was tested for contamination for the Mozambique and Tanzania sites but not for Malawi. For the current analysis, samples with MBL below 100 CFU/mL were considered negative (i.e. the lower limit of quantification [LLOQ]=100 CFU/mL) (5) and TTP above 42 days were considered negative.

Modelling strategy overview

The main goal with the model development was to develop a final model that described the relationship between MBL and TTP data. However, the model development was divided into first developing a MBL only model, after which TTP data was included in the modelling to develop a final, joint MBL-TTP model.

For the continuous MBL biomarker directly reflecting bacterial load, we considered analysing this biomarker using models able to describe declining bacterial density in sputum, such as a bi-exponential function as applied previously to MBL data (5). The model for bacterial load was termed the sputum sub-model.

The TTP data was analysed in a different fashion (8) considering it is an indirect measurement of bacterial load reflecting time-to-event data. For TTP, the experimental procedure is first to inoculate bacteria in sputum in a liquid culture where growth takes place. This was described in our approach by linking the sputum model which describes changes in bacterial load in sputum to a mycobacterial growth sub-model. The growth in liquid culture leads to carbon dioxide production and as the carbon dioxide reaches a certain level, a positive signalling event is recorded. Thus, a high degree of growth is expected to yield a high probability of achieving a short TTP and this was handled in our approach by linking the growth to the probability of a positive signalling event to occur using survival modelling by incorporating a hazard sub-model. Finally, a novel feature of this work is the addition of an additional sub-model to account for contaminated TTP samples, implemented as a probability component to describe differences in the probability of TTP contamination over time and between the different study sites.

120

121 *Modelling of MBL data*

122 The MBL data was described through a sputum sub-model describing the total bacterial load
123 in the patient's sputum. The sputum model that was used as a starting point included a single
124 mycobacterial subpopulation with exponential kill where bacterial load in sputum (B_s) over
125 time on treatment (t_t) was calculated according to:

126 $$B_s(t_t) = B_{0,s} \times e^{-k \times t_t}$$ (Eq. 1)

127 where the MBL prediction was set equal to the bacterial load (i.e. $MBL(t_t)=B_s(t_t)$). The $B_{0,s}$
128 parameter describes the initial (pre-treatment) bacterial load and k is a first-order kill rate
129 exhibited by the combination treatment. In this way, the drug effect was modelled as an
130 "on/off" treatment effect not accounting for drug concentrations, i.e. this concentration-
131 independent approach ignores pharmacokinetics. As this work developed, we tested a model
132 that included two mycobacterial subpopulations ($B1_s$ and $B2_s$, respectively) with first-order
133 rate constants for bacterial killing (k_1 and k_2, respectively) according to:

134 $$B_s(t_t) = B1_{0,s} \times e^{-k_1 \times t_t} + B2_{0,s} \times e^{-k_2 \times t_t}$$ (Eq. 2)

135 where $B1_{0,s}$ and $B2_{0,s}$ describe the initial bacterial load of B1 and B2, respectively. In addition
136 to the two subpopulation model, a three subpopulation was also tested. As a molecular
137 measure we assumed that MBL captured a total population and, thus, the prediction of MBL
138 was set to the sum of the different bacterial subpopulations in sputum. The MBL data that
139 were below the LLOQ which was set to 100 CFU/mL in this work was handled using the M3
140 method within NONMEM which is a preferred way for missing data (13).

141

142

143 *Modelling of MBL-TTP data*

144 For modelling TTP, the sputum sub-model established based on the MBL data was extended
145 with additional sub-models (a schematic representation of how the different sub-models
146 connect can be seen in Figure 1). Thus, the sputum sub-model had a central role within the
147 model, and acted as the main driver for time-varying changes in both biomarkers. The
148 starting point for model development of TTP-related sub-models was derived from a previous
149 TTP model (8). A mycobacterial growth component described bacterial growth in the liquid
150 culture. The starting point for bacterial growth (the inoculum) for each liquid culture sample
151 was the predicted bacterial load at the corresponding time-point from the sputum sub-model
152 according to:

153 $B_s(t_t = t_{sample}) \rightarrow B_c(t_c = 0)$ (Eq. 3)

154 where t_{sample} is the time-point of sampling (relative to start of treatment) and B_c is the bacterial
155 density in liquid culture and t_c is time since liquid culture inoculation. In general for
156 equations, t_t (time since start of treatment) signifies processes in the patient (e.g. bacterial
157 killing) whereas t_c (time since MGIT incolulation) mainly concerns processes within the
158 liquid culture. The existence of more than one mycobacterial subpopulation that we explored
159 for the sputum model (e.g. in Equation 2) was considered for the mycobacterial growth model
160 also in which the starting point for bacterial growth was described by Equations 4 and 5.

161 $B1_s(t_t = t_{sample}) \rightarrow B1_c(t_c = 0)$ (Eq. 4)

162 $B2_s(t_t = t_{sample}) \rightarrow B2_c(t_c = 0)$ (Eq. 5)

163 Upon exploring the existence of more than one subpopulation in the liquid culture, potential
164 qualitative differences between subpopulations were tested including different growth rates

for the subpopulations and a transfer between subpopulations. Models were also tested including the existence of a non-growing subpopulation (alongside a growing population) to explore if this could explain an expected time-varying change in the MBL vs TTP relationship (similar hypotheses exists for the CFU vs TTP relationship) (14). Exponential, logistic and Gompertz growth functions were tested.

The mycobacterial growth model was coupled to a hazard model to translate growth in the MGIT liquid culture to a probability of a positive TTP signal.

Bacterial population density inside the liquid culture was the assumed contributor to the probability of a positive TTP signal. Bacterial population was an assumed proxy for carbon dioxide production, the known driver for a positive TTP signal (in this bacteria were assumed to be growing and this carbon dioxide producing). Note that no formal distinction was made between bacterial growth and carbon dioxide production which means that the bacterial grwoth represent a combination of carbon dioxide production and bacterial growth. A scaling-parameter controlled how much each bacterium inside the liquid culture contributed to the probability of a positive signal, as seen in Equation 6.

$$h(t_c) = B_c(t_c) \times Scale \quad \text{(Eq. 6)}$$

where h is the hazard and described the instantaneous probability for a positive signalling event and Scale is a scaling-parameter controlling each bacterium's contribution to the hazard. Next, the integral of the hazard over time (H) were calculated using Equation 7.

$$H(t_c) = \int_0^{t_c} h(t_c)dt) \quad \text{(Eq. 7)}$$

The survival (S, the probability over time to remain free of a positive signalling event) was calculated by Equation 8.

$$S(t_c) = e^{-H(t_c)}$$

188 For mycobacterial growth models including more than one mycobacterial subpopulation, we
189 tested for differences in the degree of contribution to the probability of a positive TTP signal
190 for each subpopulation.

191 Developing our work further, a component for the probability of contaminated TTP samples
192 was developed. Tested models included constant (Equation 9) and linearly increasing
193 probabilities (Equation 10) of contamination over time on treatment.

194 $p_{contaminated,TTP} = p_{con,base}$ (Eq. 9)

195 $p_{contaminated,TTP} = p_{con,base} + k_p \times t_t$ (Eq. 10)

196 where $p_{contaminated,TTP}$ is the probability of a contaminated TTP sample, $p_{con,base}$ is the baseline
197 probability of a contaminated TTP sample and k_p is a linear time-varying increase of
198 probability of a contaminated TTP sample. Since the sputum sampling and testing for
199 contamination differed between the sites, models were tested where separate contamination-
200 related parameters were estimated for each site.

201 At the beginning of model development, negative TTP samples were handled within the time-
202 to-event approach using right-censoring (the standard procedure for survival modelling). This
203 was compared to a model where negative samples were handled by treating negative TTP
204 samples as a different type of data observation in a separate sub-model (10). The probability
205 of a negative TTP sample was described by an E_{max} relationship between bacterial load in
206 sputum and the probability of a negative TTP ($p_{negative,TTP}$) according to Equation 11
207 (exemplified for a two subpopulation sputum model).

208 $p_{negative,TTP} = 1 - \frac{p_{max} \times (B1_s(t_t) + B2_s(t_t))^{\gamma}}{B_{50}^{\gamma} + (B1_s(t_t) + B2_s(t_t))^{\gamma}}$ (Eq. 11)

where p_{max} is the maximal probability of a positive TTP sample, B_{50} is the bacterial load of subpopulation 1 and subpopulation 2 in sputum at which the probability of a positive TTP value is half maximal and γ is a gamma-factor for the shape of the non-linear relationship.

Covariate model

Rifampicin dose group of 35- versus 10- mg/kg was tested as a covariate on the bacterial kill rate in the sputum sub-model as well as HIV status on baseline bacterial load. Another potential covariate to evaluate would be to test if pooled versus early morning sputum samples gave different baseline bacterial load (pooled samples are known to have shorter TTP) but this was note tested in this analysis. The reasons were that a graphical exploration of the data revealed no apparent differences between baseline TTP for pooled versus early morning samples and that all samples from each site had the same sampling. This would in turn have made it difficult to separate this effect between sampling method and site or region.

Another relevant covariate would have been lung cavitation on baseline bacterial load but this information was unavailable in the current dataset.

Utility of the model

The intended real-life use of the model was evaluated by re-estimating the final combined MBL-TTP model by only using the MBL or TTP data, respectively, to explore if the final combined model can be applied to predict TTP from MBL data and *vice versa*, in trials where only MBL or TTP are collected. Note that this was an actual re-estimation (i.e. not

MAXEVAL=0) but parameters strongly associated with the biomarker left out of the estimation were fixed to that of the combined MBL-TTP model. Furthermore, the model re-estimated with TTP only data can potentially be used as a standalone TTP model to analyse future TTP only datasets (but note that this work does not include validation for prospective use *per se*). In this situation, the MBL sub-model parameters were fixed to the estimates from the combined model when estimating only TTP data and *vice versa*. The evaluation was based on graphical diagnostic plots, plausibility of parameter estimates and uncertainty in parameter estimates.

Data analysis and model evaluations

The data were analysed in NONMEM 7.4 with the importance sampling (IMP) estimation method. The Laplacian estimation method did not give stable estimation for analysing MBL and TTP simultaneously. Detailed estimation settings are listed in Supplementary data S1. Data handling and plotting were done in R 3.5.1 using Xpose 4.6.1 (15) to make diagnostic plots assisted by PsN 4.8.0 (16). Models were compared based on difference in objective function value (dOFV) using the likelihood ratio test at the 1% significance level but also based on uncertainty in model parameters.

Models were assessed graphically using visual predictive checks (VPCs). For MBL, conventional VPCs were generated which compared percentiles of observed and simulated data within the same plot. If the observed and simulated data agreed, it provided evidence that the model provided a good description of the observed data.

For TTP (time-to-event data), Kaplan-Meier VPCs (see e.g. (17)) were produced, which compared observed and simulated Kaplan-Meier curves for TTP at each week. Finally, VPCs

254 were performed for TTP versus MBL to assess if the model could mimic the observed pattern

255 (relationship) between the biomarkers.

Antimicrobial Agents and Chemotherapy

Results

Patient data

Patient baseline characteristics are summarized in Table 1. For MBL, 851 samples were analysed of which 277 samples (32.5%) were below the employed LLOQ of 100 CFU/mL. For TTP, 659 samples were analysed of which 192 samples (29.1%) were contaminated and 90 samples (13.7%) were negative (i.e. the TTP was greater than 42 days).

Sub-model for MBL data

The developed sputum model included two mycobacterial subpopulations, B1 and B2 where the treatment had exponential killing of both subpopulations where the MBL prediction was assumed to represent the total bacterial population (i.e. $MBL(t_t)=B1_s(t_t)+B2_s(t_t)$). The B1 subpopulation had greater abundancy (~99%) than B2 (~1%) at pre-treatment and the B1 subpopulation was also more easily killed than B2 (B1 killed ~3.5 times more rapidly than B2). Thus, B2 were more tolerant to treatment-induced bacterial killing which led to that B2 becoming more abundant than B1 during late treatment. A statistically significant increased kill (1.66 fold) of B1 (but not B2) by rifampicin 35 vs 10 mg/kg (p=0.002) was included in the model. The HIV covariate on initial bacterial load was not statistically significant. The MBL model gave good description of the observed data according to a VPC (Figure S1).

Inclusion of two mycobacterial subpopulations in the sputum model gave a significantly better fit to the observed data than a sputum model only including a single subpopulation ($p<0.00001$). The treatment had first-order killing of both subpopulations (included as an "on/off" treatment effect). In the final MBL sputum sub-model bacteria were assumed to be

unable to grow or transfer between subpopulations in sputum. A three subpopulation model was not supported by the data as it resulted in an unstable estimation.

Inclusion of inter-individual variability in initial bacterial load of both subpopulations (B1 and B2), also including a correlation between the subpopulations led to a significantly better fit to the observed data and was therefore included in the final model.

The final model for MBL with an intended use of modelling future MBL only datasets, referred to as the standalone MBL model is given in Supplementary data S2. Parameter estimates are shown in Supplementary data S3.

Combined MBL-TTP model

The structure of the final combined MBL-TTP model is shown in Figure 1. The dynamics of each sub-model are shown for baseline and week 12 samples in addition to week 4 (which was considered relevant since it's located in the transition between the initial rapid decline and the later slower decline for bacterial load in sputum) for a typical individual in Figure 2. The final combined MBL-TTP model included the same sputum model as described above for the standalone MBL model. The same subpopulations as described within the sputum model existed within the mycobacterial growth model where only the B1 population could grow. However, B2 bacteria were able to transfer into B1 in the liquid culture (Figure 1). The model component for contaminated TTP samples included a linear relationship between time on treatment and risk of contamination. Finally, the model included a component for negative TTP including a non-linear (E_{max}) relationship between bacterial load in sputum and probability of negative TTP. Figure 3 compares sample loss due to negative and/or contaminated samples for TTP vs MBL. The figure shows that both MBL and TTP have similar degree of negative samples (Figure 3a) but due to the much higher contamination of

TTP (Figure 3b), the MBL assay gives more information in terms of non-contaminated, positive samples (Figure 3c).

Simulated data from the final combined MBL-TTP model gave good description of the observed data which showed that the model was appropriate given the data. A plot of observed and model-predicted TTP vs MBL shows that the final model accurately described the observed pattern between the biomarkers (Figure 4). A VPC of MBL vs time (Figure 5) and a Kaplan-Meier VPC of TTP vs time in liquid culture for different treatment weeks (Figure 6) also showed that the model described the observed data well. Parameter estimates of the final combined MBL-TTP model are shown in Table 2. Precision looked fine for all parameters. All parameters were estimated on linear scale.

For the mycobacterial growth model only B1 could grow but B2 could transfer into B1. A transfer rate parameter (k_{21}) described the transfer between B2 and B1 and was set to the same value as the growth rate (k_G). Estimation of a unique k_{21} led to an unstable model and was not statistically significant (p=0.176). The growth function that best described the growth of B1 was found to be the Gompertz model.

Bacterial growth was linked to the probability of a positive TTP signal using a time-to-event approach where only B1 contributed to the probability (hazard) of a positive signal (since B2 was non-growing B2 do not contribute directly to hazard). The contribution of each B1 bacterium to the probability of a positive signal was determined by a scaling-parameter. The scaling-parameter was time-varying in the final model where the value decreased exponentially from a baseline value down to a steady state value. Having a similar time-varying component for other potentially relevant parameters, such as the growth rate (k_G) or introducing a lag-time for growth, did not lead to a stable model.

The model for contaminated samples was different between sites. However, parameters estimated from the Tanzania site were considered the most appropriate model. For Tanzania, the observed contamination rate was low initially (~10%) and increased linearly to reach a contamination rate of ~60% by week 12. For Malawi, contamination was not determined (i.e. no blood agar test was done). For Mozambique, contamination was moderately high (~30-40%) across all time-points. A VPC for contamination vs time (Figure S2) confirmed that the model gave a good description of the observed contamination data.

A sub-model was included in the final model to handle negative TTP. The probability of a negative sample increased as bacterial load in sputum decreased (10). An inhibitory sigmoidal E_{max}-model described the relationship where the lowest possible probability of a negative sample was estimated to be 3.3% and occurred at a very high bacterial density. The probability of a negative sample was half-maximal at a bacterial density of 48.8 CFU/mL. This is a rather low number which represents roughly half the LLOQ of 100 CFU/mL which was used in this analysis for MBL. A model where negative TTP samples were handled using right-censoring within the hazard model (which is common practice for time-to-event models) did not lead to an acceptable description of the observed data and was therefore discarded.

Inter-individual variability was included for the scaling-parameter that accounted for the contribution of B1 to the probability of a positive signalling event in the liquid culture.

Utility of the final model

It was possible to re-estimate the final combined MBL-TTP model using only MBL data if the TTP-related parameters were fixed to the parameters of the final model, where the model gave good description of the observed MBL data (Figure S3). The final model with the TTP-related parameters fixed can be found in Supplementary data S2. Likewise, we successfully re-

estimated the final model with only TTP data with MBL-related parameters fixed to the final model estimates with good fit to the observed data (Figure S4). The model estimated with TTP only data can be used as a standalone TTP model to estimate TTP only datasets. The final MBL-TTP model with the MBL-related parameters fixed can be found in Supplementary data S2.

A comparison of parameter estimates for the final combined MBL-TTP model estimated including all data, the final model re-estimated with MBL or TTP data only and the standalone MBL model can be found in Supplementary data S3. There was consistency in the estimated parameters between all the models. The covariate effect of enhanced performance of 35 mg/kg rifampicin was estimable using all models, i.e. using MBL or TTP data only as well as with all data.

360 **Discussion**

361 This analysis describes the development of a pharmacometric model to identify the
362 relationship between two critical measures of viable count; MBL and TTP based on data
363 collected during 12 weeks in drug-susceptible TB patients treated with the standard drug
364 combination. In this model the relationship between the biomarkers was identified
365 successfully.

366 To make an effective model it was necessary to include components that described the
367 different data types; MBL is a continuous variable whereas TTP is a time-to-event variable
368 indirectly reflecting bacterial load. The best sputum model (describing the underlying
369 bacterial load in sputum) was achieved when we included two mycobacterial subpopulations
370 (B1 and B2) with treatment resulting in an exponential fall in viable count for both. The
371 predicted MBL was assumed to be the total bacterial population in sputum (i.e.
372 $MBL(t_t)=B1_s(t_t)+B2_s(t_t)$). Although the drug effect was included as an "on/off" treatment
373 effect which represents a limitation of the present study, in the future it can/will be replaced
374 by exposure-response relationships in later analyses. In our model the B1 subpopulation was
375 more abundant than B2 at pre-treatment whereas B2 became more abundant than B1 on late
376 treatment days since B1 was killed more rapidly than B2. This is similar to the report of
377 Honeyborne *et al*. (5) although their work only included MBL data. We agree with their
378 analysis that the B2 population may represent persisters (5). A three subpopulation model
379 was tested during the model development. A three subpopulation model reflective of
380 multiplying, semi-dormant and persister cells would have been a more mechanistically
381 plausible structure compared to the two subpopulations described in this work as TB is known
382 to exist in at least three subpopulations (18). To interpret these results we may need to
383 consider that the B1 and B2 subpopulations may also partly contain semi-dormant cells
384 although to what extent this occurs is unknown. This also had implications when exploring

385 the relationship between MBL and TTP; with only two subpopulations included we were not
386 able to appropriately explore our hypothesis that MBL reflects more bacterial subpopulations
387 than TTP (i.e. we could not explore if TTP quantified semi-dormant but not persister cells
388 without semi-dormant cells in the model). According to the final model structure both
389 subpopulations contributed to MBL and TTP which can be interpreted as that both biomarkers
390 reflect the same subpopulations. However, we do not have this view of our results, we still
391 hypothesize that MBL may reflect more subpopulations than TTP and that our results just
392 confirm that there is a large overlap in what subpopulations each biomarker captures. Yet we
393 found that the three subpopulation model was not stable although the reasons for this are
394 unknown.

395 However, one potential explanation to the instability is that the clinical data used for this
396 analysis contained a sub-optimal number of "critical" data points where persisters are
397 expected to be the dominating subpopulation which we believe occur primarily at late time-
398 points (Figure 3). If a lower MBL LLOQ than 100 CFU/mL is applied in a future analysis it
399 may lead to more critical data points. Another option where critical persister-dominated data
400 points can be studied in controlled settings could be *in vitro* systems. Alternatively, the MBL
401 information can be supplemented with information from staining-based techniques to identify
402 phenotypic resistance based on lipid bodies (19), a study that is currently underway.

403 An important advance in this model is the way in which it includes a sub-model that allowed
404 us to predict TTP in a mechanistically plausible manner (Figure 1). The sputum model acted
405 as the fundamental hub within the model where changes in the predicted bacterial load in
406 sputum affected both the resulting MBL and TTP predictions. As anticipated, the relationship
407 between MBL and TTP lies in the sputum model. The most essential way that the sputum
408 model affected the TTP predictions was through the mycobacterial growth model describing
409 growth in liquid culture as well as the hazard model which described how growth affected the

probability of a positive signal. This way of linking sub-models has been described in other time-to-event models only describing TTP data (8–10). Although the general structure of our model is similar to previous reports, what makes our model unique is the description of two distinct bacterial subpopulations both in the sputum model and in the mycobacterial growth model. The underlying study had no experimental data which could distinguish between the two populations, this was instead described by the mathematical model. In the liquid culture, B2 was non-growing but could indirectly contribute to growth by transferring into B1 potentially reflecting a shift to a more metabolically active state triggered by the nutrient-rich liquid culture media. The transfer rate of B1 transferring to B2 (k_{21}) was set to the same value as the bacterial growth rate (k_G). This was reasonable given the insufficient data to inform differences in these parameters. Furthermore, when the mycobacterial growth model was linked to the hazard model which translates the growth in the liquid culture to a probability of a positive signal, only B1 contributed to the probability of a positive TTP. As the underlying reason for a positive signalling is carbon dioxide production this implies that non-growing B2 bacteria do not contribute measurably to carbon dioxide production. Both findings, i.e. that B2 is non-growing and do not produce carbon dioxide were driven by the data and are important observations. It may explain a disproportionally greater TTP prolongation on early versus late treatment days as not only the MGIT inoculum decrease each week, the proportion of bacteria that can grow and readily produce carbon dioxide immediately upon liquid culture inoculation has also decreased (i.e. the B1/B2 ratio decrease with treatment time). This observation agrees with and provide further insight into a hypothesis generated in a non-model-based analysis comparing CFU, time to appearance of CFU and TTP (20). In that study (20) there was significant correlation between time to appearance of the first CFU colony on solid media and TTP suggesting that the fastest growing bacteria has a disproportionally larger contribution to the carbon dioxide production in liquid culture, i.e. a similar interpretation as can be drawn

435 from our work. Another finding within our model that also contributes to this relationship is
436 the time-varying scaling-parameter which decreased with time on treatment. The time-varying
437 scaling parameter is, once again, a data-driven finding. Future *in vitro* work should explore
438 the biological explanation.

439 Previous models have treated TTP as a continuous variable (21–24). Our work suggests that
440 this is not the optimal way to handle these data as time-to-positivity reflects time-to-event
441 data. As was the case for a previous publication, a time-to-event analysis of TTP revealed an
442 exposure-response relationship of rifampicin (8) that was undetected for the same dataset
443 when the TTP data was treated as continuous data (25).

444 One of the challenges of modelling data from TB clinical trials is that previously published
445 MGIT-TTP models lack components for contamination, which is a significant confounder of
446 this assay. Thus, the contamination sub-model is a significant improvement on the previously
447 published models for TTP since it allows for real-world clinical trial simulations. Our model
448 can be used to make simulations prior to performing clinical TTP studies to predict the degree
449 of TTP sample loss. We regard the predicted and observed degrees of contamination as high
450 (Figure 3) suggesting that TTP can be unreliable and difficult to interpret, especially during
451 late treatment thus, making it meaningful to get a reliable expectation on the degree of sample
452 loss. Significantly, it means that MBL, which is not affected by contamination is a significant
453 improvement over TTP as shown in Figure 3. The typical patient is expected to have greater
454 sample loss for TTP than MBL when accounting for both contamination and negative
455 samples. The included component for contaminated TTP was based on time on treatment and
456 was site-dependent but we recommend the contamination model derived from Tanzania for
457 performing clinical trial simulations since contamination for Tanzania data started low at
458 baseline and increased with time on treatment, which represents the most plausible
459 contamination pattern. It has been shown that during early treatment patients produce sputum

of better quality than later on treatment where patients get healthier which is associated with a relative inability to produce sputum (26).

A sub-model was included to describe negative TTP samples which predicted that lower bacterial densities in sputum gave higher probability of a negative TTP sample. This way of handling negative TTP samples is similar as a previous model for TTP (10). An E_{max} model described this relationship (Figure 2e) and predicted a probability of a negative TTP of 3.3% at very high bacterial densities suggesting that a fraction of TTP samples will always be negative. The model by Svensson and Karlsson (10) predicted that 3.1% will always be negative which is similar to our value.

The developed model gave good fit to the observed data according to the diagnostic plots in Figures 4-6. In addition, the parameter precision in the parameters was overall low (Table 2). This shows that from a technical model validation perspective, the presented model is valid.

In this work we identified a statistically significant increased (1.66 fold) killing effect for 35 vs 10 mg/kg rifampicin which indicates that the joint collection of MBL and TTP data used along with our modelling approach is a powerful strategy for detecting inter-regimen differences for Phase IIb trials. If studies are designed and analysed according to our approach Phase IIb trial performance may be simplified and could require fewer patients to be recruited. However, this was based on data from 12 patients and the model as such was not tested on any external data.

The utility analysis showed that the model can be used to analyse MBL data alone to predict TTP and *vice versa* if parameters related to the excluded biomarker are fixed according to Supplementary data S3. We argue that using the model in this way should be valid for data from drug-susceptible TB patients. However, for drug-resistant TB the bacterial killing may be slower and initial bacterial load as well as growth rate in liquid culture may deviate and

studies investigating this are required. One of the most encouraging aspects of this model is that the parameter for difference in bacterial kill for 35 vs 10 mg/kg rifampicin was identifiable when using data from one or the other biomarker or when using data from both.

The original study (11) which reports the underlying data had not gone through formal peer-review by the time of manuscript submission of the present work.

The developed pharmacometric model predicted a general trend of lower probability of TTP culture conversion at week 8 for higher bacterial loads compared to lower bacterial loads. This conclusion could probably not have been drawn as easily directly from the observed data. In the observed data the mean baseline TTP was 5.7 days for patients with culture negativity at week 8 and the mean baseline TTP was 6.0 for patients with culture positivity at week 8. For other time-points (including weeks 1, 4 and 6), the mean TTP was also similar between patients with and without culture conversion at week 8. However, for week 2 there mean TTP was higher for patients with culture negativity at week 8 (15.6 days) compared to patients with culture positivity at week 8 (9.8 days).

In conclusion, our work reports a practical combined MBL-TTP model that relates the changing bacterial load for both markers. We also developed two sub-models that can be used to analyse TTP and MBL separately. The combined MBL-TTP model can be used to predict TTP from MBL data and *vice versa* and could be used to re-analyse historical trials. We confirm and delineate the extent that MBL gives higher proportion of positive samples than TTP due to high proportion of contaminated TTP samples. The standalone MBL model can be used to analyse clinical trials where exposure-response of drugs and regimens quantified with only MBL is of interest.

506 **Acknowledgements**

507 The data presented here came from PANBIOME project funded by the European Developing
508 Countries Clinical Trials Partnership (EDCTP) grant: SP.2011.41304.008 (Molecular
509 biomarkers in MAMS trial). The authors thank all members of the PANBIOME consortium,
510 particularly the African partner sites that have implemented the molecular monitoring of anti-
511 tuberculosis treatment.

512

513 **References**

514 1. Diacon AH, van der Merwe L, Demers A-M, von Groote-Bidlingmaier F, Venter A,
515 Donald PR. 2014. Time to positivity in liquid culture predicts colony forming unit
516 counts of Mycobacterium tuberculosis in sputum specimens. Tuberc Edinb Scotl
517 94:148–151.

518 2. Gosling RD, Heifets L, Gillespie SH. 2003. A multicentre comparison of a novel
519 surrogate marker for determining the specific potency of anti-tuberculosis drugs. J
520 Antimicrob Chemother 52:473–476.

521 3. Diacon AH, Maritz JS, Venter A, van Helden PD, Dawson R, Donald PR. 2012. Time to
522 liquid culture positivity can substitute for colony counting on agar plates in early
523 bactericidal activity studies of antituberculosis agents. Clin Microbiol Infect 18:711–
524 717.

525 4. Sabiiti W, Ntinginya N, Kuchaka D, Azam K, Kampira E, Mtafya B, Bowness R, Bhatt
526 N, Davies G, Kibiki G, Gillespie S. 2017. Molecular Bacterial Load Assay: A Fast and
527 Accurate Means for Monitoring Tuberculosis Treatment Response. BMJ Glob Health
528 2:A8–A8.

529 5. Honeyborne I, McHugh TD, Phillips PPJ, Bannoo S, Bateson A, Carroll N, Perrin FM,
530 Ronacher K, Wright L, van Helden PD, Walzl G, Gillespie SH. 2011. Molecular
531 bacterial load assay, a culture-free biomarker for rapid and accurate quantification of
532 sputum Mycobacterium tuberculosis bacillary load during treatment. J Clin Microbiol
533 49:3905–3911.

534 6. Gillespie SH, Sabiiti W, Oravcova K. 2017. Mycobacterial Load Assay. Methods Mol
535 Biol Clifton NJ 1616:89–105.

7. Honeyborne I, Mtafya B, Phillips PPJ, Hoelscher M, Ntinginya EN, Kohlenberg A, Rachow A, Rojas-Ponce G, McHugh TD, Heinrich N, Pan African Consortium for the Evaluation of Anti-tuberculosis Antibiotics. 2014. The molecular bacterial load assay replaces solid culture for measuring early bactericidal response to antituberculosis treatment. J Clin Microbiol 52:3064–3067.

8. Svensson RJ, Svensson EM, Aarnoutse RE, Diacon AH, Dawson R, Gillespie SH, Moodley M, Boeree MJ, Simonsson USH. 2018. Greater Early Bactericidal Activity at Higher Rifampicin Doses Revealed by Modeling and Clinical Trial Simulations. J Infect Dis 218:991–999.

9. Chigutsa E, Patel K, Denti P, Visser M, Maartens G, Kirkpatrick CMJ, McIlleron H, Karlsson MO. 2013. A time-to-event pharmacodynamic model describing treatment response in patients with pulmonary tuberculosis using days to positivity in automated liquid mycobacterial culture. Antimicrob Agents Chemother 57:789–795.

10. Svensson EM, Karlsson MO. 2017. Modelling of mycobacterial load reveals bedaquiline's exposure-response relationship in patients with drug-resistant TB. J Antimicrob Chemother 72:3398–3405.

11. Sabiiti W, Azam K, Kuchaka D, Mtafya B, Bowness RE, Oravcova K, Farmer E, Honeyborne I, Evangelopoulos D, McHugh TD, Xiao H, Khosa C, Rachow A, Heinrich N, Kampira E, Davies G, Bhatt N, Ntinginya N, Viegas S, Jani I, Kamdolozi M, Mdolo A, Khonga M, Boeree MJ, Philips PP, Sloan DJ, Hoelscher M, Kibiki G, Gillespie SH. 2019. Improving diagnosis and monitoring of treatment response in pulmonary tuberculosis using the molecular bacterial load assay (MBLA). bioRxiv 555995 available from https://www.biorxiv.org/content/10.1101/555995v1.

559 12. Boeree MJ, Heinrich N, Aarnoutse R, Diacon AH, Dawson R, Rehal S, Kibiki GS,
560 Churchyard G, Sanne I, Ntinginya NE, Minja LT, Hunt RD, Charalambous S, Hanekom
561 M, Semvua HH, Mpagama SG, Manyama C, Mtafya B, Reither K, Wallis RS, Venter A,
562 Narunsky K, Mekota A, Henne S, Colbers A, Balen GP van, Gillespie SH, Phillips PPJ,
563 Hoelscher M. 2017. High-dose rifampicin, moxifloxacin, and SQ109 for treating
564 tuberculosis: a multi-arm, multi-stage randomised controlled trial. Lancet Infect Dis
565 17:39–49.

566 13. Beal SL. 2001. Ways to fit a PK model with some data below the quantification limit. J
567 Pharmacokinet Pharmacodyn 28:481–504.

568 14. Bowness R, Boeree MJ, Aarnoutse R, Dawson R, Diacon A, Mangu C, Heinrich N,
569 Ntinginya NE, Kohlenberg A, Mtafya B, Phillips PPJ, Rachow A, Plemper van Balen G,
570 Gillespie SH. 2015. The relationship between Mycobacterium tuberculosis MGIT time
571 to positivity and cfu in sputum samples demonstrates changing bacterial phenotypes
572 potentially reflecting the impact of chemotherapy on critical sub-populations. J
573 Antimicrob Chemother 70:448–455.

574 15. [http://xpose.sourceforge.net/] (accessed on 19/03/01).

575 16. [https://uupharmacometrics.github.io/PsN/] (accessed on 19/03/01).

576 17. Plan E. Pharmacometric methods and novel models for discrete data. Uppsala University
577 2011 Available from: http://urn.kb.se/resolve?urn=urn:nbn:se:uu:diva-150929 Accessed
578 15 Jul 2019.

579 18. Coates ARM, Hu Y. 2008. Targeting non-multiplying organisms as a way to develop
580 novel antimicrobials. Trends Pharmacol Sci 29:143–150.

581 19. Hammond RJH, Baron VO, Lipworth S, Gillespie SH. 2018. Enhanced Methodologies
582 for Detecting Phenotypic Resistance in Mycobacteria. Methods Mol Biol Clifton NJ
583 1736:85–94.

584 20. Barr DA, Kamdolozi M, Nishihara Y, Ndhlovu V, Khonga M, Davies GR, Sloan DJ.
585 2016. Serial image analysis of Mycobacterium tuberculosis colony growth reveals a
586 persistent subpopulation in sputum during treatment of pulmonary TB. Tuberc Edinb
587 Scotl 98:110–115.

588 21. Diacon AH, Dawson R, Hanekom M, Narunsky K, Maritz SJ, Venter A, Donald PR, van
589 Niekerk C, Whitney K, Rouse DJ, Laurenzi MW, Ginsberg AM, Spigelman MK. 2010.
590 Early bactericidal activity and pharmacokinetics of PA-824 in smear-positive
591 tuberculosis patients. Antimicrob Agents Chemother 54:3402–3407.

592 22. Sloan DJ, Mwandumba HC, Garton NJ, Khoo SH, Butterworth AE, Allain TJ,
593 Heyderman RS, Corbett EL, Barer MR, Davies GR. 2015. Pharmacodynamic Modeling
594 of Bacillary Elimination Rates and Detection of Bacterial Lipid Bodies in Sputum to
595 Predict and Understand Outcomes in Treatment of Pulmonary Tuberculosis. Clin Infect
596 Dis Off Publ Infect Dis Soc Am 61:1–8.

597 23. Kayigire XA, Friedrich SO, van der Merwe L, Donald PR, Diacon AH. 2015.
598 Simultaneous staining of sputum smears for acid-fast and lipid-containing
599 Myobacterium tuberculosis can enhance the clinical evaluation of antituberculosis
600 treatments. Tuberc Edinb Scotl 95:770–779.

601 24. Burger DA, Schall R. 2015. A Bayesian Nonlinear Mixed-Effects Regression Model for
602 the Characterization of Early Bactericidal Activity of Tuberculosis Drugs. J Biopharm
603 Stat 25:1247–1271.

604 25. Boeree MJ, Diacon AH, Dawson R, Narunsky K, du Bois J, Venter A, Phillips PPJ,
605 Gillespie SH, McHugh TD, Hoelscher M, Heinrich N, Rehal S, van Soolingen D, van
606 Ingen J, Magis-Escurra C, Burger D, Plemper van Balen G, Aarnoutse RE, PanACEA
607 Consortium. 2015. A dose-ranging trial to optimize the dose of rifampin in the treatment
608 of tuberculosis. Am J Respir Crit Care Med 191:1058–1065.

609 26. Karinja MN, Esterhuizen TM, Friedrich SO, Diacon AH. 2015. Sputum volume predicts
610 sputum mycobacterial load during the first 2 weeks of antituberculosis treatment. J Clin
611 Microbiol 53:1087–1091.

612

613 **Figures legends**

614 **Figure 1** Schematic representation of the final combined MBL-TTP model. The treatment is
615 represented by an "on/off" effect i.e. the drugs kill the bacteria in the presence of drugs. The
616 killing of bacteria, represented by two mycobacterial sub-populations in the sputum ($B1_s$ and
617 $B2_s$) is governed by two first-order kill-rates (k_1 and k_2) in the sputum model. The sum of $B1_s$
618 and $B2_s$ constitutes the MBL sub-model and gives the prediction of MBL (MBL model,
619 lowest middle box). The predicted bacterial densities of the sub-populations in sputum ($B1_s$
620 and $B2_s$) are the inoculum for the mycobacterial growth model (top middle box), at the
621 corresponding sampling time point. Only $B1_c$ in the liquid culture has the ability to grow. The
622 $B2_c$ cannot grow but can transfer into the $B1_c$ subpopulation with a first-order rate of k_{21}. A
623 TTP model (top right box) translates the growth within the mycobacterial growth model to a
624 positive TTP signal where only $B1_c$ contributes to the probability of a positive TTP signal.
625 This is done using survival modelling, where $B1_c$ multiplied by a time-varying factor accounts
626 for the relative contribution of each $B1_c$ bacterial cell to the probability of a positive signal.
627 Negative TTP samples are described by a non-linear (E_{max}) relationship between the bacterial
628 density in sputum ($B1_s$+$B2_s$) and probability of a negative TTP sample (upper middle box).
629 Contaminated TTP samples are described by a function for the probability of a contaminated
630 sample that increase linearly with time on treatment (lower middle box).

631 Abbreviations: k_1; first-order bacterial kill rate of bacterial sub-population $B1_s$, k_2; first-order
632 bacterial kill rate of bacterial sub-population $B2_s$, MBL; molecular bacterial load, TTP; time-
633 to-positivity,

634

635 **Figure 2** Typical model predictions within each component of the final combined MBL-TTP
636 model for a patient treated with isoniazid, pyrazinamide, ethambutol and 10 mg/kg rifampicin.

637 The (a) panel shows predictions from the sputum model where the line represents the
638 prediction of MBL. The (b) panel shows predictions of the bacterial density in the liquid
639 culture. Remaining panels show the predicted time-varying probability of not having a
640 positive TTP signal (c), probability of contaminated TTP samples (d) and probability of
641 negative TTP samples (e). The different symbols in panels (a), (d) and (e) show the dynamics
642 within the corresponding sub-model where circles represent an early baseline sample, squares
643 represent an intermediate (4-week) sample and triangles represent a late (week 12) sample. In
644 panels (b) and (c), the circles represent an early (baseline) sample, the squares represent an
645 intermediate (4-week) sample and the triangles represent a late (week 12) sample.

646 Abbreviations: MBL; molecular bacterial load, TTP; time-to-positivity

647

648 **Figure 3** Sample loss for MBL (filled circles) and TTP (filled triangles) due to (a) negative
649 samples, i.e. assuming no loss of samples due to contamination, (b) contaminated samples,
650 assuming no loss of samples due to negativity and (c) total sample loss reflecting the
651 combined sample loss due to negative samples and contaminated samples.

652 Abbreviations: TTP; time-to-positivity, MBL; molecular bacterial load

653

654 **Figure 4** The relationship between TTP and MBL. The VPC shows the median (solid line)
655 and 5^{th} and 95^{th} percentiles (lower and upper dashed lines, respectively) of observed data
656 compared to the corresponding percentiles of simulated data (shaded areas) based on 1000
657 simulated datasets where lighter grey are percentiles and darker grey is median. The open
658 circles show the actual observations.

Abbreviations: TTP; time-to-positivity, MBL; molecular bacterial load, VPC; visual predictive check

Figure 5 Visual predictive check (VPC) for the MBL data using the final combined MBL-TTP model. The VPC shows the median (solid line) and 5th and 95th percentiles (lower and upper dashed lines, respectively) of observed data compared to the corresponding percentiles of simulated data (shaded areas) where lighter grey are percentiles and darker grey is median. The open circles show the actual observations and the dotted line is the lower limit of quantification for MBL. The shaded areas represent 95% confidence interval of simulated data based on 1000 simulated datasets.

Abbreviations: MBL; molecular bacterial load

Figure 6 Kaplan-Meier visual predictive check (VPC) of the TTP data using the final combined MBL-TTP model. The VPC shows the observed Kaplan-Meier (survival) curve for each weeks' TTP as solid lines and the simulated Kaplan-Meier 95% confidence intervals are shown as blue shaded areas (n=1000 simulated datasets).

Abbreviations: TTP; time-to-positivity, MGIT; mycobacterial growth incubator tube

674 **Tables**

675 Table 1 – Baseline patient characteristics for all data and by study site

Parameter	All sites (n=105)	Malawi (n=20)	Mozambique (n=53)	Tanzania (n=32)
Weight (kg)	54 (37-74)	55.8 (43-70)	54.0 (37-74)	-
Male sex (n)	77 (73%)	14 (70%)	35 (66%)	28 (88%)
HIV positive (n)	45 (42.9%)	9 (45.0%)	36 (67.9%)	0 (0%)
Rifampicin 10 mg/kg (n)	93 (89%)	20 (100%)	53 (100%)	20 (63%)
Rifampicin 35 mg/kg (n)	12 (11%)	0 (0%)	0 (0%)	12 (38%)
Baseline TTP (days)	4.22 (1.02-23.1)	6.02 (3.14-16.10)	4.13 (2.00-9.60)	3.21 (1.02-23.1)
Negative baseline TTP (n)[a]	2 (1.90%)	0 (0%)	2 (3.77%)	0 (0%)
Baseline MBL (log10 CFU/mL)	5.91 (2.62-8.37)	5.43 (3.61-7.83)	6.35 (2.62-8.28)	5.26 (3.04-8.37)
Negative baseline MBL (n)[b]	1 (0.95%)	0 (0%)	1 (1.89%)	0 (0%)

676 Data are median values (ranges) or no. (%) of patients.

677 [a]Defined as a TTP longer than 42 days [b]Defined as a log10 MBL value below 2

678 Abbreviations: TTP; time-to-positivity, MBL; molecular bacterial load

679

680

681 Table 2 – Parameter estimates of the final combined MBL-TTP model

Parameter	Description	Estimate
Sputum model		
$B1_{0,s}$ (CFU/mL)	Initial bacterial load of mycobacterial subpopulation 1 in sputum	0.365×10^{6} (28.8)
k_1 ($week^{-1}$)	First-order bacterial kill rate of subpopulation 1 in sputum	1.71 (8.70)
$B2_{0,s}$ (CFU/mL)	Initial bacterial load of mycobacterial subpopulation 2 in sputum	0.00430×10^{6} (51.4)
k_2 ($week^{-1}$)	First-order bacterial kill rate of subpopulation 2 in sputum	0.494 (9.50)
$Dose_{35mg}$	Fold increase in bacterial killing of k_1 by 35 versus 10 mg/kg rifampicin	1.66 (14.0)
IIV $B1_{0,s}$ (%)	Inter-individual variability in $B1_{0,s}$	239 (9.18)
IIV $B2_{0,s}$ (%)	Inter-individual variability in $B2_{0,s}$	227 (10.9)
Corr $B1_{0,s}$ – $B2_{0,s}$ (%)	Correlation between $B1_{0,s}$ and $B2_{0,s}$	45.4 (15.6)
ε (%)	Additive error on log scale for MBL data	79.7 (4.96)
Mycobacterial growth model		
k_G (day^{-1})[a]	Mycobacterial growth of subpopulation 1 in liquid culture	0.395 (8.50)
k_{21} (day^{-1})[a]	Transfer rate from subpopulation 2 to subpopulation 1 in liquid culture	0.395 (8.50)
B_{max} (CFU/mL)	Maximal bacterial load in liquid culture	166×10^{6} (24)
TTP model		
$Scale_{BL}$	Baseline value of scaling parameter accounting for the contribution of subpopulation 1 bacteria to the probability of a positive TTP signal	6.68×10^{-9} (31.6)
IIV $Scale_{BL}$ (%)	Inter-individual variability in $Scale_{BL}$	80.6 (18.1)
$Scale_{SS}$	Steady state value of scaling parameter	0.601×10^{-9} (24.3)
k_S ($week^{-1}$)	First-order rate constant for time-varying change of the scaling parameter	1.28 (25.1)
Model for negative TTP samples		
p_{max}	Maximal probability of a positive TTP sample	0.967 (1.50)
B_{50}	Bacterial load of subpopulation 1 and subpopulation 2 in sputum at which the probability of a positive TTP value is half maximal	49.8 (33.7)
γ	Gamma-factor for non-linear E_{max} relationship for negative TTP samples	0.756 (18.9)
Model for contaminated TTP samples		
$p_{con,base}$[c]	Baseline probability of a contaminated TTP sample	0.0910 (39.0)
k_p[c]	Linear time-varying increase of probability of a contaminated TTP sample	0.0416 (13.9)

682 The reported values are the final estimates with relative standard error (RSE) shown in brackets as the
683 approximate coefficient of variation (%CV) on standard deviation scale. The IIV and residual error are shown as
684 the approximate %CV on standard deviation scale (calculated using a simple square-root formula,
685 %CV=100×√(variance)). Correlation (Corr $B1_{0,s}$ – $B2_{0,s}$) is reported as the percentage correlation coefficient.

686 The mathematical structure for the final model was as follows (final NONMEM code in Supplementary data S2):

687 $B1_s(t_t) = B1_{0,s} \times e^{-k_1 \times t_t \times \mathrm{Dose}_{35mg}}$ (B1 subpopulation in sputum)

688 $B2_s(t_t) = B2_{0,s} \times e^{-k_2 \times t_t}$ (B2 subpopulation in sputum)

689 where Dose_{35mg} is 0 for 10 mg/kg rifampicin and the individually predicted MBL=$B1_s(t_t)$+$B2_s(t_t)$

690 $\frac{dB1_c}{dt_c} = B1_c(t_c) \times k_G \times \log\left(\frac{B_{max}}{B1_c(t_c)+B2_c(t_c)}\right) + k_{21} \times B2_c(t_c)$ (B1 subpopulation in liquid culture)

691 $\frac{dB2_c}{t_c} = -B2_c(t_c)$ (B2 subpopulation in liquid culture)

692 where the initial conditions for each TTP sample were $B1_c(t_c = 0) = B1_s(t_t = sampling\ time\ point)$ and
693 $B2_c(t_c = 0) = B21_s(t_t = sampling\ time\ point)$ for the B1 and B2 subpopulations, respectively

694 $h(t_c) = B1_c(t_c) \times (Scale_{BL} + (Scale_{SS} - Scale_{BL}) \times (1 - e^{-k_S \times t_t}))$ (TTP model)

695 where the cumulative hazard ($H(t_c) = \int_0^{t_c} h(t_c)dt$) were used to calculate the survival ($S(t_c) = e^{-H(t_c)}$)

696 $p_{contaminated,TTP} = p_{con,base} + k_{con} \times t_t$ (model for contaminated TTP samples)

697 $p_{negative,TTP} = 1 - \frac{p_{max} \times (B1_s(t_t)+B2_s(t_t))^{\gamma}}{B_{50}^{\gamma}+(B1_s(t_t)+B2_s(t_t))^{\gamma}}$ (model for negatvie TTP samples)

698 [*]Final parameter estimates of the MBL standalone model, the model predicting TTP based on MBL and the
699 model predicting MBL based on TTP are available in Supplementary data S3.

700 [a]k_{21} and k_G were modelled as a single parameter in the model, [b]The parameters for contaminated TTP samples
701 were estimated on data from Tanzania, the other sites included time-constant probabilities of 0 for Malawi (fixed
702 value, since contamination was not measured) and 0.336 (10.0% RSE) for Mozambique

703 Abbreviations: TTP; time-to-positivity, t_t; time on treatment, MBL; molecular bacterial load, t_c; time in liquid
704 culture, $p_{contaminated,TTP}$; probability for a contaminated TTP sample, $p_{negative,TTP}$; probability for a negative TTP
705 sample

706

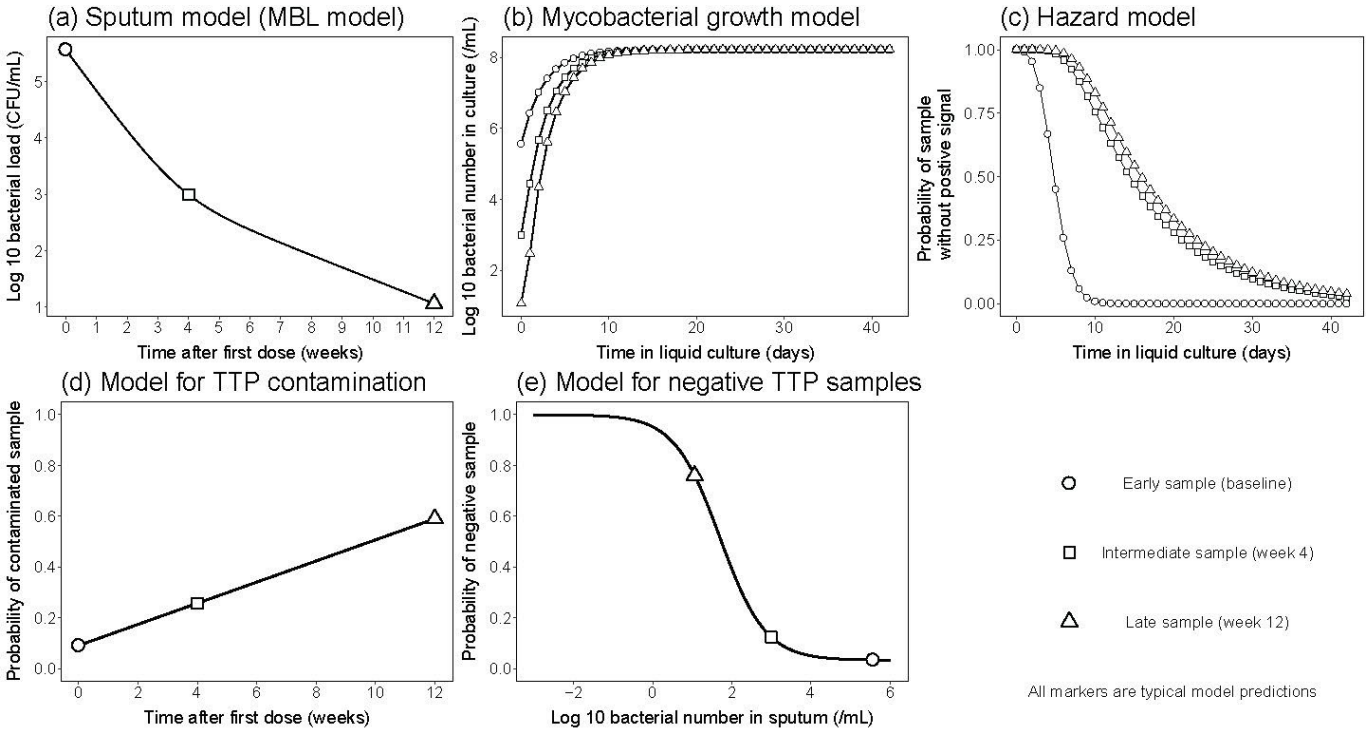

Antimicrobial Agents and Chemotherapy

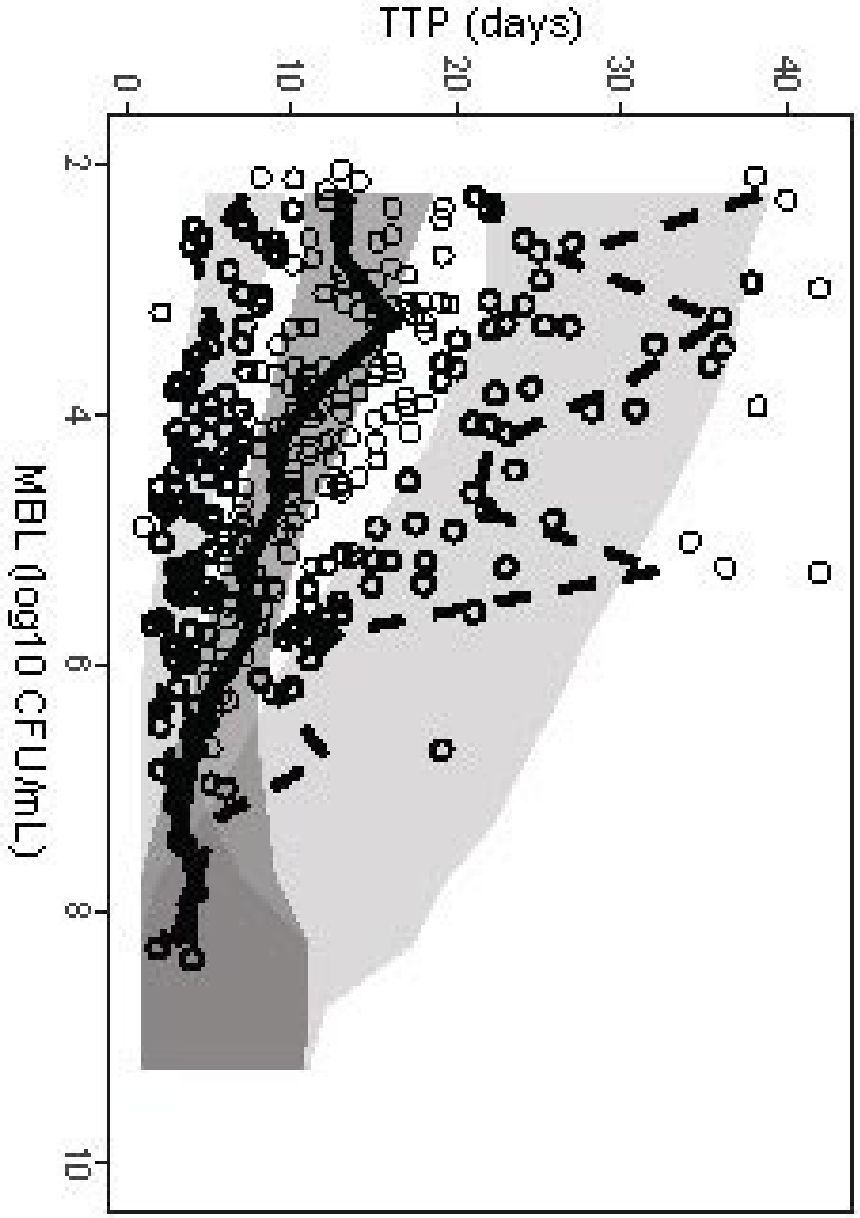

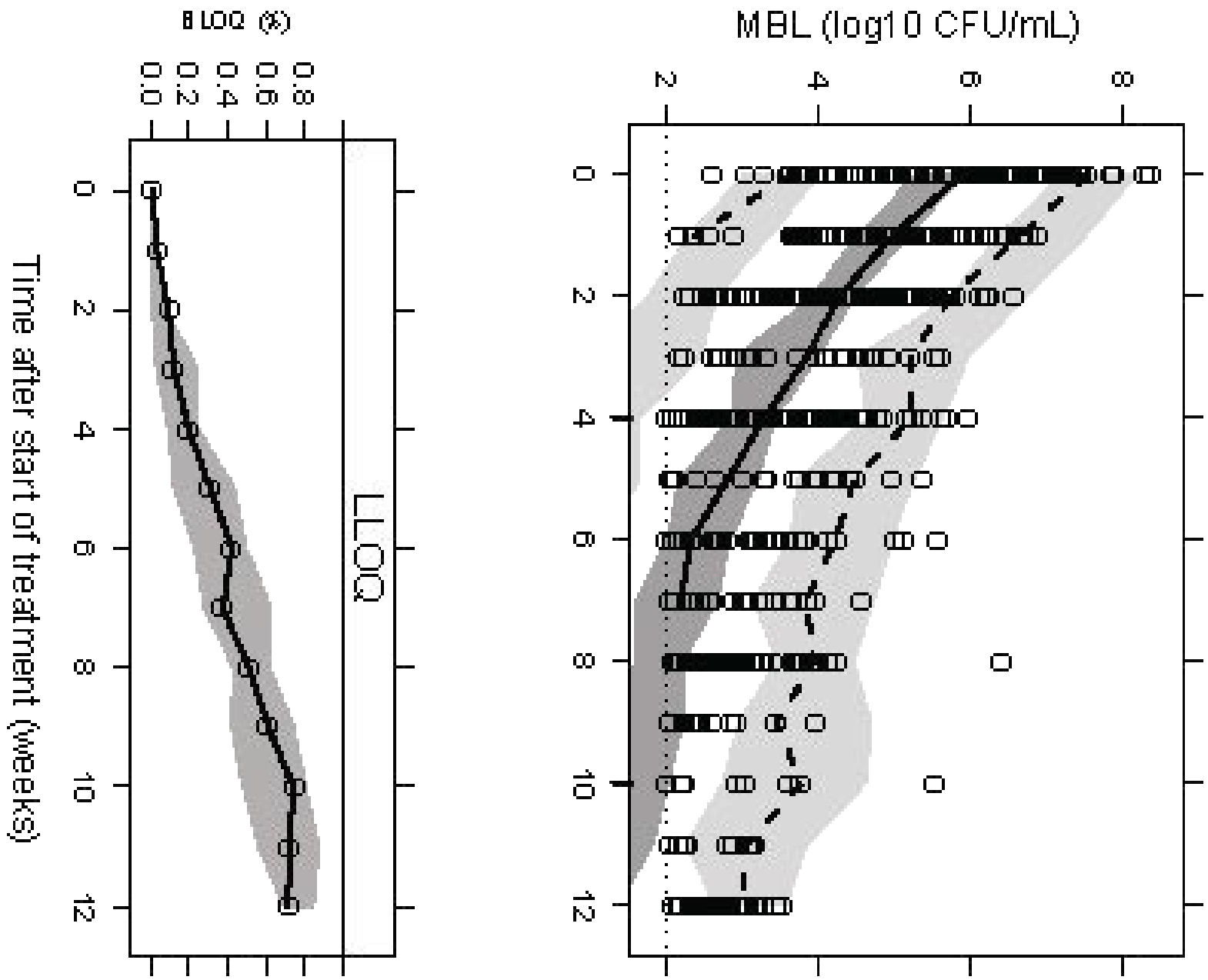

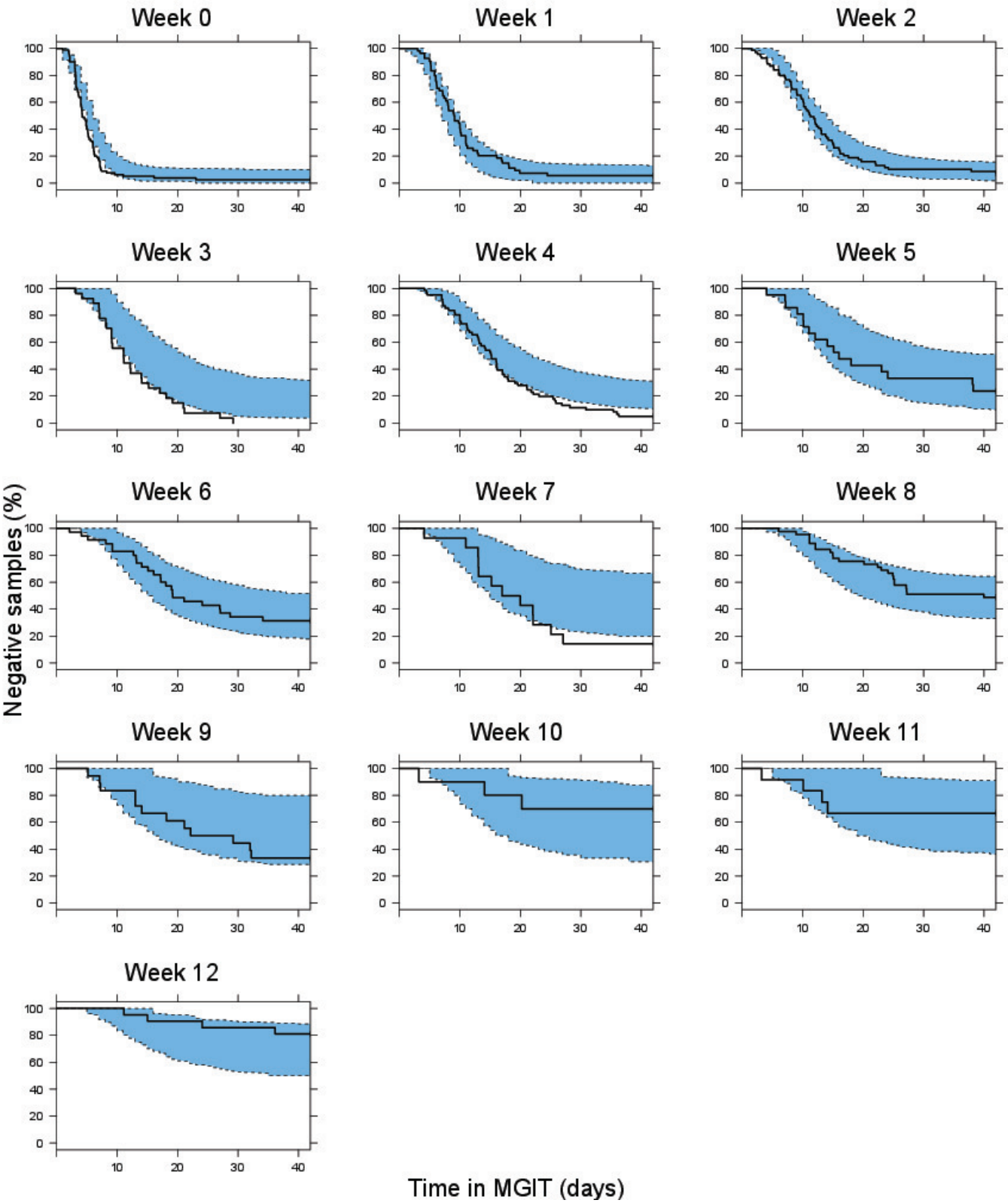

Antimicrobial Agents and Chemotherapy